Proceedings of the 7th International Conference on Materials Chemistry and Environmental Engineering
DOI: 10.54254/2755-2721/2027.39059

Review of Origami-Inspired Modular Thick-Panel Origami Deployable Structures (MUTOIS)

Shangkun Deng[1,*], Zhixiang Hu[2], Ziao Lu[3]

[1]Department of Materials Science and Engineering, Leeds Joint School, Southwest Jiaotong University, Chengdu, China
[2]Xi'an Gaoxin No.1 High School, Xi'an, China
[3]Harrow Beijing, Beijing, China
**Corresponding Author. Email: gjkg0945@leeds.ac.uk*

Abstract. Real-world material thickness imposes constraints that spatial mechanisms cannot ignore—physical joints must move without binding, and the overall geometry has to stay compatible throughout deployment. Working within the Modular and Uniformly Thick Origami-Inspired Structures (MUTOIS) framework, Degree-6 (D6) and Degree-10 (D10) vertices were evaluated through a combination of cardstock/MDF physical prototyping and Denavit-Hartenberg (D-H) kinematic formulations. From benchtop load trials, it was found that spatial symmetry enables the overconstrained D6 node to preserve a rigid single-DOF folding trajectory. For the D10 configuration, four internal degrees of freedom were identified; while its geometry does provide clearance against facet collisions, the joint network still tends to bind under manual actuation. Connecting two modules together introduces angle-dependent non-linear torque at the inter-unit interfaces, and the operational mobility drops from a theoretical M=9 to an effective M_{eff}=4. These empirical results offer concrete kinematic guidelines for choosing between different node types in thick-panel deployable lattices.

Keywords: Modular origami, Thick-panel deployable structures, Kinematic analysis, Degree-6 vertex, Multi-DOF mechanisms

1. Introduction

Origami-inspired deployable architectures are valued for their high packaging efficiency and excellent stiffness-to-weight performance, which explains their appeal in space structures and adaptable building applications [1, 2]. However, to realize these advantages with actual engineering materials, spatial interference and hinge binding must be dealt with—problems that emerge as soon as solid thick plates take the place of ideal zero-thickness creases [3]. Over the years, various ways have been proposed to accommodate panel thickness t : shifting hinge lines, beveling panels, adopting kirigami-style cutouts, or using 3D-printed flexural hinges.

© 2026 The Authors. This is an open access article distributed under the terms of the Creative Commons Attribution License 4.0 (https://creativecommons.org/licenses/by/4.0/).

DOI: 10.54254/2755-2721/2027.39059

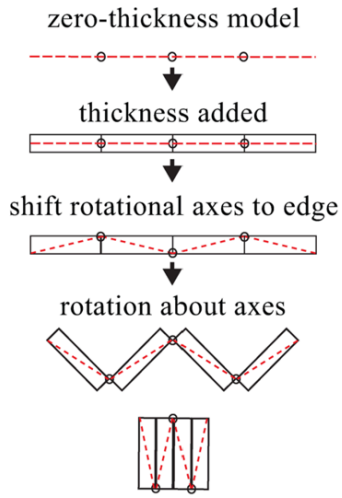


Figure 1. Representative mechanism for panel thickness accommodation. An illustrative schematic demonstrating the hinge shift strategy designed to mitigate kinematic jamming during folding [2]

As illustrated in Figure 1, shifting the rotational axes to the panel edges serves as a representative strategy to mitigate kinematic jamming during folding.

Zhu and Filipov [4] recently provided a mathematical treatment for Modular and Uniformly Thick Origami-Inspired Structures (MUTOIS) [4]. From their loop-closure, developability, and flat-foldability equations, it follows that only 6-crease and 10-crease vertices can meet the rigid closure requirements under uniform thickness:

$$\prod_{i=1}^{N} T_i = I_{4\times4}\ (Spatial\ loop-closure\ mechanism) \tag{1}$$

$$\sum_{i=1}^{N} a_i = 0\ (Developability\ condition) \tag{2}$$

$$a_1 + a_3 + \ldots + a_{N-1} = a_2 + a_4 + \ldots + a_N\ (Flat\text{-}foldability\ condition) \tag{3}$$

Here T_i accounts for both the rotation about the crease line and the translational offset required by the uniform panel thickness t.

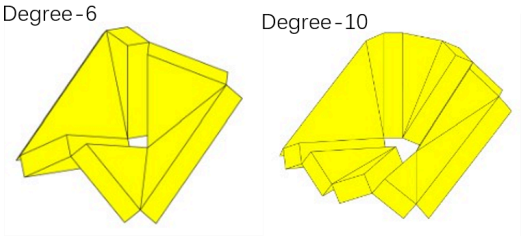


Figure 2. Thick origami vertices with 6 and 10 creases

As depicted in Figure 2, the Degree-6 and Degree-10 configurations form the basic building blocks under this uniform thickness constraint.

There is often a gap between what ideal rigid-origami solvers predict and what actually happens during physical deployment [5, 6]. This discrepancy comes from joint friction, hinge compliance, non-uniform manual actuation, and torque distribution across the interfaces [7]. To evaluate physical

DOI: 10.54254/2755-2721/2027.39059

performance, benchtop experiments were combined with closed-loop numerical simulations—specifically, physical D6 and D10 thick-panel assemblies were built and tested to quantify kinetic stability, multi-DOF binding, non-linear torque amplification, and the effective mobility reduction seen in coupled modular arrays [8].

2. Experimental methodology and model design

2.1. Retrospective model analysis

$$M = 6(N - J - 1) + \sum_{i=1}^{J} f_i \tag{4}$$

The kinematic feasibility of the D6 thick-panel model was first checked by treating it as an overconstrained 6R linkage. For an arbitrary 1-DOF spatial closed chain, the Kutzbach criterion normally calls for $N = 7$ links; a 6-link assembly ($N = 6 < 7$) thus gives $M = 6(6 - 6 - 1) + 6(1) = 0$. On top of that, the thick-panel loop-closure equations ($T_1 \cdots T_6 = I$) introduce six independent constraints—three rotational and three translational—which would imply an immobile structure ($DOF = N - 6 = 0$) [9]. For a D10 node, however, $N = 10 > 7$, and the mobility works out to $M = 6(10 - 10 - 1) + 10(1) = 4$ DOFs. Being a multi-degree-of-freedom (MDOF) mechanism by its very nature, this configuration is inherently harder to control during deployment.

The Supplementary Information (SI) goes into more detail about how the theoretical locking in the D6 node can be overcome, allowing it to function as an overconstrained 1-DOF mechanism with a single folding path [4]. In practical terms, fabrication has to focus on preserving the geometric conditions that make this possible: enforcing spatial symmetry to pair rotation axes, matching cut angles and joint offsets (d_i) accurately so that twist-angle compatibility holds ($\alpha_1 = \alpha_3 = \alpha_5, \alpha_2 = \alpha_4 = \alpha_6$), and reducing the six independent loop-closure equations to five to release the desired SDOF motion [7]. For MDOF systems like D10, attention must also be paid to reliable fixation, structural rigidity, uniform panel thickness for easy connection, and enough fill-in panels to maintain the essential thick-panel kinematics [10].

2.2. Physical prototyping



Figure 3. Material preparation for thick-panel prototypes

DOI: 10.54254/2755-2721/2027.39059

The prototypes were built out of medium-density fiberboard (MDF) panels, using cardboard strips as the hinge substrate and paper strips as flexible joint elements. Tape was applied to bond the paper strips to the panels and reinforce the hinge lines [11]. A cardboard knife was used for straight cuts, while rulers and protractors helped keep the planned dimensions and angles on track.

Figure 3 demonstrates the raw material preparation and panel cutting process for the thick-panel prototypes.

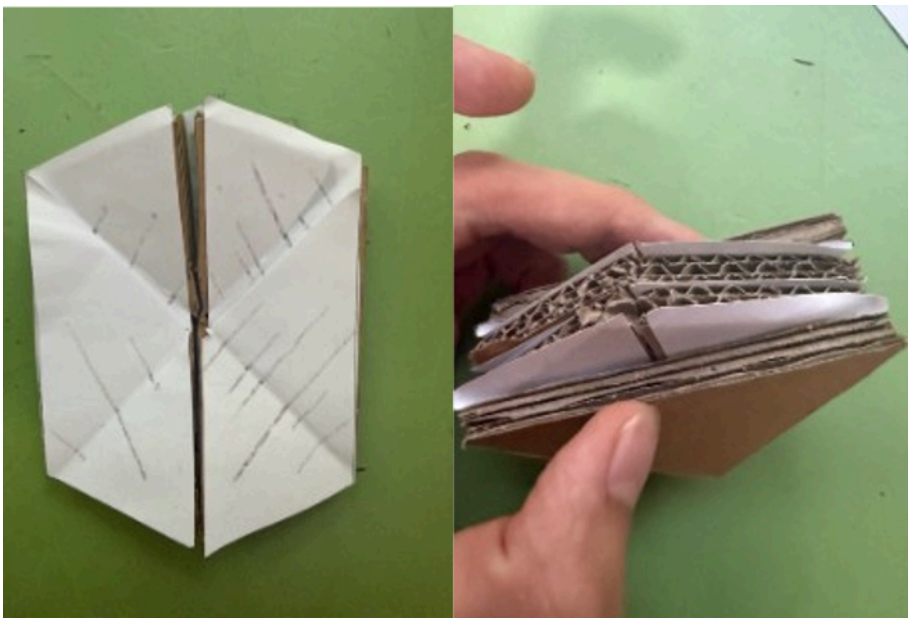


Figure 4. Unfolded and folded state of the Degree-6 prototype

The Degree-6 (D6) and Degree-10 (D10) MUTOIS prototypes were both produced using the same manual workflow. Heavy cardstock sheets were marked and cut into six and ten identical triangular facets, respectively, with steel straightedges and protractors ensuring accurate geometry. For the flexible revolute joints, 2-cm-wide paper strips were taped across the seams between adjacent panels, aligning each strip's centerline with the crease axis before closing the facets into a continuous spatial ring. When the two were compared on the benchtop, the differences in kinematic stability were striking. Pushing inward manually along opposite panel edges—or applying symmetric four-corner actuation—made the overconstrained D6 prototype repeatedly follow a deterministic single-degree-of-freedom (SDOF) deployment path, with no bifurcation or binding. Adding four more facets to create the D10 node, though, brought in multi-DOF compliance; even with the same joint preparation procedure, the D10's higher mobility made its folding trajectory highly sensitive to asymmetric hand-driving. These tests show that while uniform-thickness fabrication methods work for both vertex orders, only the symmetric D6 geometry consistently delivers robust and predictable SDOF performance under unscripted manual inputs. Figure 4 shows the unfolded and folded state of the Degree-6 prototype, and Figure 5 shows the unfolded and folded state of the Degree-10 prototype.

As shown in Figure 4, the D6 prototype transitions smoothly between its unfolded and fully folded states.

DOI: 10.54254/2755-2721/2027.39059

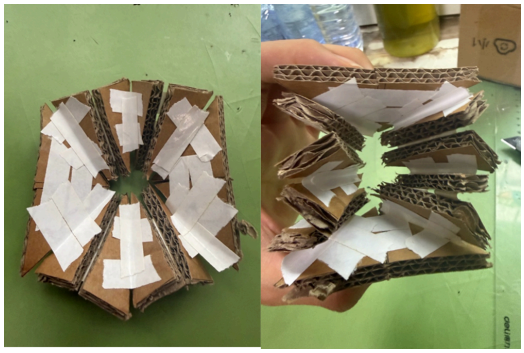


Figure 5. Unfolded and folded state of the Degree-10 prototype

Figure 5 depicts the unfolded and folded states of the Degree-10 prototype, highlighting its increased panel count and complex spatial geometry.

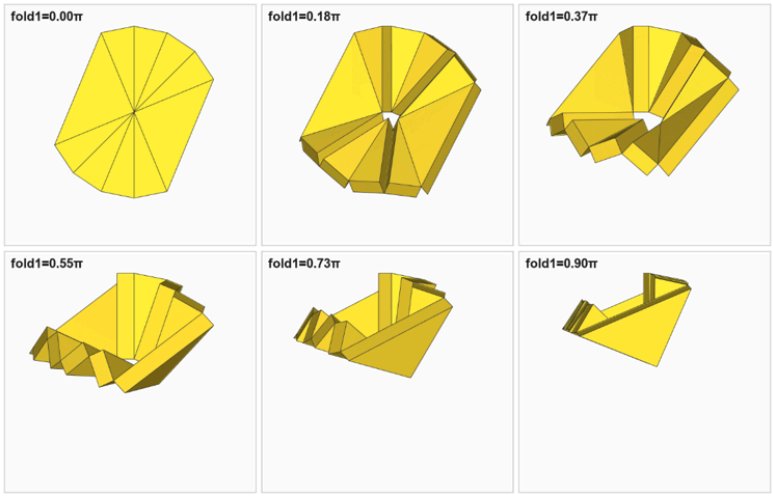


Figure 6. Numerical folding simulation of the Degree-10 vertex

The multi-DOF nature and complex panel layout of the Degree-10 (D10) module make it difficult to follow the spatial folding progression just by looking at the physical model. Therefore, before fabrication, a MATLAB kinematic simulation was run using D-H matrix closure equations.

As presented in Figure 6, the continuous deployment from 0.00π (flat) to 0.90π (folded) tracks how the geometry evolves and how the vertex complies kinematically throughout the numerical simulation.

3. Results and discussion

3.1. Degree-6: over-constrained single-path stability

Testing the Degree-6 configuration bore out what the mobility analysis suggested—it follows a deterministic single-degree-of-freedom folding path. Under symmetric driving, the prototype repeated the same deployment trajectory run after run, and the kinematic response stayed stable throughout. Repeated folding did produce minor wear near the crease lines (also mentioned in the SI) [4], but the structure as a whole remained intact. This kind of localized wear is a useful reminder that classical theoretical models have to assume rigid panels and frictionless hinges, which is never

DOI: 10.54254/2755-2721/2027.39059

quite true in practice. That aside, the empirical evidence confirms that the overconstrained Degree-6 vertex offers a predictable, low-maintenance mechanism—one that fits nicely with the needs of deployable systems.

3.2. Degree-10: multi-DOF complexity and engineering limitations

The Degree-10 prototype, by comparison, posed some real control difficulties. With four degrees of freedom active, the structure requires coordinated force inputs across all creases; any imbalance in actuation led to binding or deviation from the intended path. Motion tracking showed visible oscillation and high sensitivity to how the driving force was applied—a clear sign that mathematical closure does not by itself guarantee smooth physical operation. While the larger clearance between panels does prevent geometric interference, it does not translate into any measurable performance gain over the Degree-6 node [12]. From an engineering standpoint, these observations back the choice of Degree-6 as the primary MUTOIS building block: it offers the best compromise among functional folding, structural robustness, and ease of fabrication.

4. Multi-module interconnectivity and coupling kinematics

Connecting Degree-6 and Degree-10 unit cells into a larger spatial lattice creates an interconnected network whose behavior is shaped by coupled kinematic constraints. What was found from testing these combined modules is that the interfaces between units do not lock the whole array into a rigid, deterministic motion pattern. Instead, the connections allow some local decoupling: one cell can fold all the way down while its neighbor stays flat, which helps avoid premature binding at the joints. However, rotating the connection axes between modules relative to each other has a marked effect on the overall deformation pattern and how forces are transmitted through the joints. Under non-orthogonal mounting angles, the inter-unit hinges show non-linear torque amplification, and this changes substantially how external driving forces make their way through the panel assembly [8]. Figure 7 shows the inter-module coupling hinge design, and Figure 8 shows the kinematic coupling and torque amplification in multi-vertex arrays.



Figure 7. Inter-module coupling hinge design

As shown in Figure 7, a customized inter-module coupling hinge was designed to connect adjacent units.

DOI: 10.54254/2755-2721/2027.39059

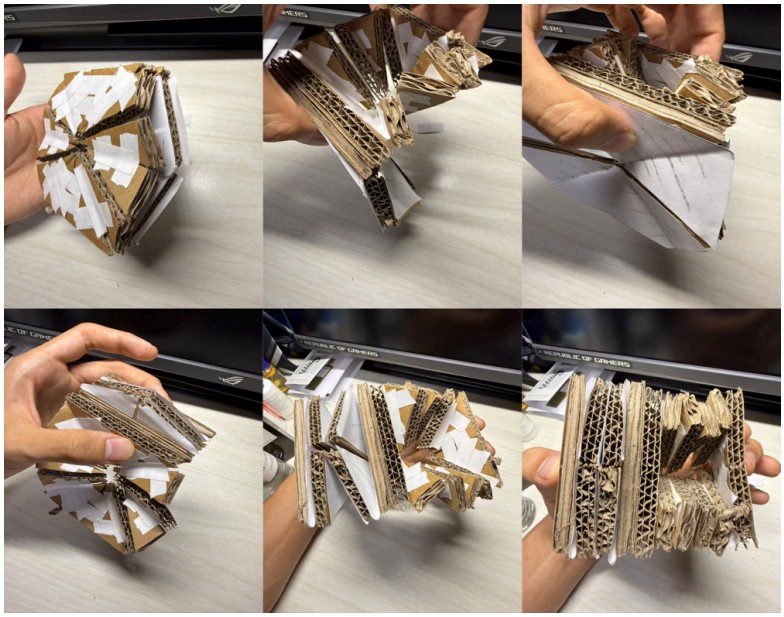


Figure 8. Kinematic coupling and torque amplification in multi-vertex arrays

Figure 8 illustrates the kinematic coupling and torque amplification observed across multi-vertex arrays during continuous deployment.

To quantify this dynamic coupling theoretically, the 3D Kutzbach criterion was extended to the two-module combined assembly,which has $N = 15$ rigid facets and $J = 15$ single-DOF revolute hinges sharing a central seam:

$$M_{\text{coupled, theoretical}} = 6(15 - 15 - 1) + 15(1) = 6(-1) + 15 = 9 \text{ DOFs}$$

This rigid-body calculation gives nine mathematical degrees of freedom, but when the assembly was actually actuated on the benchtop, substantial internal motion suppression was observed. Interface alignment constraints and spatial planar symmetry knock out five internal rotational modes during manual folding, leaving an effective mobility of $M_{\text{eff}} = 4$. Interestingly, this number matches the kinematic freedom of a standalone D10 node. This indicates that multivertex MUTOIS arrays do not simply add up independent DOFs; instead, they are limited by the most flexible component in the assembly [4, 8].

$$M_{\text{coupled, theoretical}} = 6(15 - 15 - 1) + 15 = 9 \longrightarrow M_{\text{eff}} = 4$$

5. Conclusions

Putting physical prototypes on the benchtop and running D-H kinematic simulations side by side makes one thing clear: Degree-6 and Degree-10 thick-panel vertices behave in fundamentally different ways. The over constrained D6 relies on geometrical symmetry to deliver a deterministic single-DOF folding path—predictable, no jamming, straightforward to deploy. The under constrained D10, on the other hand, brings four active freedoms along with it, and that translates into trajectory uncertainty and actuation sensitivity when driven manually. Hook them up in multi-

DOI: 10.54254/2755-2721/2027.39059

module arrays, and the spatial alignment between units pulls the theoretical mobility down from $M = 9$ to an effective $M_{\text{eff}} = 4$, while non-linear torque shows up along the coupling seams. The overall picture that emerges is this: for modular deployable structures, low-DOF nodes—especially D6—give you better motion predictability and more reliable static stability.

Acknowledgement

The authors would like to express their deepest gratitude to Professor Zhong You for his invaluable academic supervision, strategic guidance, and continuous encouragement throughout this research. Special thanks are extended to research mentor Keyao Song for his insightful technical discussions, hands-on guidance, and substantial feedback on the manuscript. In addition, the authors gratefully acknowledge Southwest Jiaotong University (SWJTU) for providing the academic platform and collaborative environment that supported the Neoschool Project. No specific funding was received for this work.

References

[1] Filipov, E. T., Tachi, T., & Paulino, G. H. (2015). Origami tubes assembled into stiff, yet reconfigurable structures and metamaterials. *Proceedings of the National Academy of Sciences, 112*(40), 12321–12326.
[2] Lang, R. J., Nelson, T. G., Magleby, S. P., & Howell, L. L. (2018). A review of thickness-accommodation techniques in origami-inspired engineering. *Applied Mechanics Reviews, 70*(1), 010805.
[3] Misseroni, D., Pratapa, P. P., Liu, K., Kresling, B., Chen, Y., Daraio, C., & Paulino, G. H. (2024). Origami engineering. *Nature Reviews Methods Primers, 4*(1), 40.
[4] Zhu, Y., & Filipov, E. T. (2024). Large-scale modular and uniformly thick origami-inspired adaptable and load-carrying structures. *Nature Communications, 15*(1), 2353.
[5] Chen, Y., Peng, R., & You, Z. (2015). Origamics of thick panels. *Science, 349*(6246), 396–400.
[6] Tachi, T. (2009). Generalization of rigid origami roofs. *Proceedings of the International Association for Shell and Spatial Structures (IASS)*, 2287–2298.
[7] Yang, J., Zhang, X., Chen, Y., et al. (2022). Folding arrays of uniform-thickness panels to compact bundles with a single degree of freedom. *Proceedings of the Royal Society A, 478*, 20220043.
[8] Fan, Z., Wang, R., Huang, H., et al. (2024). Design and analysis of an origami-inspired modular thick-panel deployable structure. *International Journal of Mechanical Sciences, 282*, 109579.
[9] Zhao, C., Cui, E., Zou, S., et al. (2025). One-degree-of-freedom flat-foldable thick-panel origami-kirigami structures: Modular arrays and closed polyhedra. *Communications Engineering, 4*, 62.
[10] Melancon, D., Gorissen, B., Garcia-Mora, C. J., et al. (2021). Multistable inflatable origami structures at the metre scale. *Nature, 592*(7855), 545-550.
[11] Ye, H., et al. (2023). Multimaterial 3D printed self-locking thick-panel origami metamaterials. *Nature Communications, 14*, 1607.
[12] Peng, R., & Chirikjian, G. S. (2025). Thick-panel origami structures forming seamless surfaces. *Nature Communications, 16*(1), 3141.